stellarator news

Published by Fusion Energy Division, Oak Ridge National Laboratory
Building 9201-2 P.O. Box 2009 Oak Ridge, TN 37831-8071, USA

Editor: James A. Rome Issue 78 November 2001
E-Mail: jar@ornl.gov Phone (865) 574-1306
On the Web at *http://www.ornl.gov/fed/stelnews*

Ballistic transport in TJ-II

Cold pulse propagation studies [1] were carried out at the TJ-II stellarator [2] (B_0 < 1.2 T, R = 1.5 m, and a = 0.22 m). For this purpose, a fast injection system was installed. Nitrogen was injected in short (<10-ms) pulses, and the total amount injected was varied by means of the voltage to the gas valve and the pressure in the line, thus allowing control of the effect on the plasma. The nitrogen radiation was observed to remain located near the edge, while the 8-channel electron cyclotron emission (ECE) electron temperature diagnostic detected the inward propagation of a temperature drop (cold pulse).

The analysis concentrated on the arrival of the cold front (the time at which the temperature begins to change), this being a strictly perturbative effect because at this time the background plasma has not yet been affected.

The cold pulse front was found to propagate "ballistically," i.e., at a roughly constant velocity (Fig. 1). The pulse front remained sharp in time (unlike diffusive propagation), and the propagation could not be well modeled by using a simple one-dimensional (1-D) diffusion model that included a pinch term. The propagation speed was of the order of 20 m/s in the outer half of the plasma and increased to around 80 m/s in the inner half, in contrast to diffusive propagation, which would slow down.

Both the plasma potential and the fluctuation level observed by the Langmuir probes in the external part of the plasma were modified significantly (the fluctuation level dropped by a factor of 3, possibly because of a decrease in the edge gradients). Using a Mirnov coil, it was found that a 40-kHz MHD mode was destabilized at the instant the cold pulse front arrived at the central region of the plasma, indicating that the MHD mode was localized at a central position. Likewise, the 2-mm scattering diagnostic (sensitive to k-values of 3 and 6 cm^{-1}), operating at a normalized radius of ρ = 0.6, observed a significant change of signal level at the time of passage of the cold pulse front. The presence of an MHD mode was also seen on Thomson scattering pressure profiles taken before

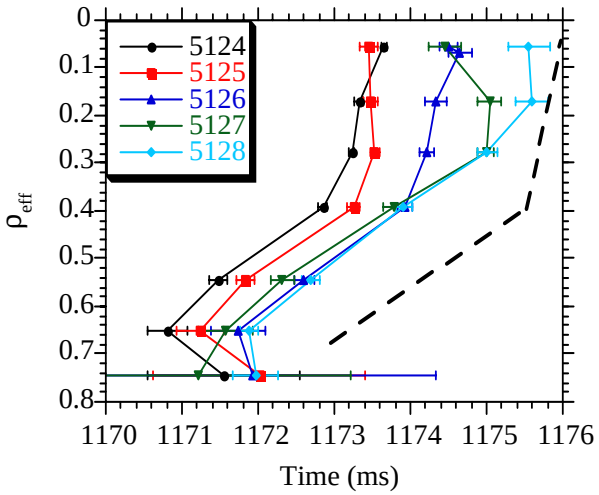

Fig. 1. Time of arrival of the cold pulse front at various radial locations in five successive shots.

In this issue . . .

and after the pulse, and the central part of the pressure profile was found to be significantly narrower after the pulse.

In these experiments, small spontaneous central electron temperature spikes, probably related to the interaction between strongly localized electron cyclotron resonant heating (ECRH) heating and a central value of rotational transform ι that is close to a rational value, produced small heat pulses propagating outward. Although these outward pulses were too small to support firm conclusions about their ballistic or diffusive nature, their propagation speed was very similar to that of the cold pulse front reported above. This phenomenon occurred in the same discharges as the cold pulse experiments. The simultaneous observation of propagating pulses in both directions is remarkable and inconsistent with a pinch term in the transport equation, which might otherwise be invoked to partially explain rapid propagation phenomena.

The observations indicate that the "fast" (i.e., non-diffusive) propagation of the cold pulse front is related to the successive activation of instabilities at certain rational surfaces. This seems to support the ideas put forward in Refs. [3] and [4]. In order to investigate this possibility further, growth rates and mode widths were estimated using a resistive interchange instability code in toroidal geometry [5] with pressure profiles similar to the experimental profiles. A rough estimate of the propagation velocity by this mechanism (successive destabilization of modes) was found to be in agreement with the experimentally observed propagation velocity, and moreover was capable of explaining the central acceleration, as a result of the steep central pressure gradient (Fig. 2). The proposed mechanism fits well in the general framework of self-organized criticality (SOC) models.

Further experiments are planned to substantiate this idea. For example, varying the instability threshold (the magnetic well), should have a significant influence on the propagation velocity of cold pulses.

B. Ph. van Milligen, E. de la Luna, F. L. Tabarés,
E. Ascasíbar, T. Estrada, F. Castejón, J. Castellano, I. García-Cortés, J. Herranz, C. Hidalgo, J. A. Jimenez, F. Medina, M. Ochando, I. Pastor, M. A. Pedrosa, and D. Tafalla
Laboratorio Nacional de Fusión por Confinamiento Magnético
Asociación Euratom-CIEMAT
28040 Madrid, Spain

L. García, R. Sánchez
Departamento de Física
Universidad Carlos III
28911 Madrid, Spain

A. Petrov, K. Sarksian, N. Skvortsova
General Physics Institute, Russian Academy of Sciences
Ulitsa Vavilova 38
Moscow, 199911 Russia

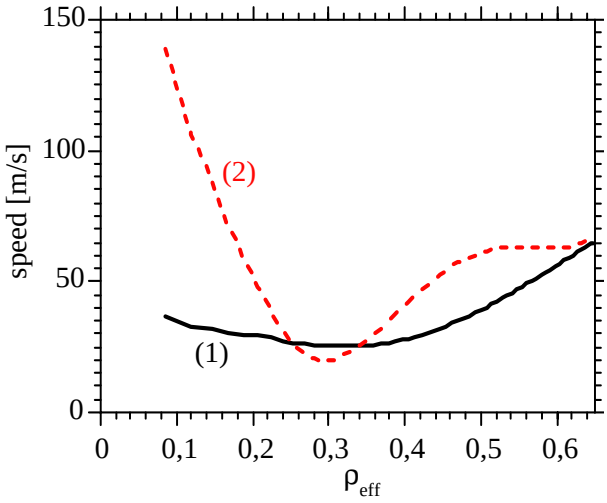

Fig. 2. Theoretical pulse propagation speed obtained using smoothed Thomson scattering pressure profiles (1) before and (2) after the cold pulse.

References

[1] B. Ph. van Milligen, E. de la Luna, F. L. Tabarés, et al., "Ballistic transport phenomena in TJ-II," Submitted to Nuclear Fusion (2001).

[2] C. Alejaldre et al., Plasma Phys. Controlled Fusion **41** A539 (1999) .

[3] B. A. Carreras, D. Newman, V. E. Lynch, and P. H. Diamond, "A model realization of self-organized criticality for plasma confinement," Phys. Plasmas **3** (8), 2903 (1996).

[4] P. H. Diamond and T. S. Hahm, "On the dynamics of turbulent transport near marginal stability," Phys. Plasmas **2** (10), 3640 (1996).

[5] L. García, B. A. Carreras, and V. E. Lynch, "Spatiotemporal structure of resistive pressure-gradient driven turbulence," Phys. Plasmas **6** (1), 107 (1999).

Attainment of 10-keV central electron temperatures in LHD by ECH

One of the main objectives of the Large Helical Device (LHD) is to extend the plasma confinement database for helical systems. Among the various plasma parameter regimes, the study of confinement properties in the collisionless regime is of particular importance since neoclassical transport theory predicts that the plasma confinement in helical devices is degraded in the low collisionality regime, but it also predicts that this degradation can be mitigated by the presence of a radial electric field.

In the current (fifth) LHD experimental campaign, the goal is to explore the high electron temperature, low electron density regime using an upgraded electron cyclotron resonance heating (ECH) system. A high central electron temperature (T_{e0} exceeding 10 keV) has been achieved by direct local ECH using a strongly focused Gaussian beam at the fundamental and second harmonic resonances.

ECH system and magnetic configuration

The ECH system has been routinely operated since the first plasma production in LHD. The gyrotrons and transmission lines have been upgraded step by step. The gyrotrons are now at 82.7 and 84 GHz for the fundamental heating and 168 GHz for the second harmonic heating.

Towards the end of the previous (fourth) experimental campaign, six sets of gyrotrons, transmission lines, and antennas were operated simultaneously, resulting in a total injected power more than 1 MW for 0.5 s. During the preparation period between the fourth and fifth experimental campaigns, two collector potential depression (CPD) type diode gyrotrons delivering 700 kW at 84 GHz with Gaussian beams were installed. One of them is connected to the newly installed evacuated 1.25-inch corrugated waveguide transmission system, and the other is attached to a conventional 3.5-inch waveguide system.

Another major improvement that contributed to the attainment of high electron temperature is the modification of the steering range. Figure 1 shows the injection beam, Mod-*B* contours, and flux surfaces in the vertically elongated poloidal cross section. The microwave sources used are two 84-GHz CPD gyrotrons, two 82.7-GHz non-CPD gyrotrons, and three 168-GHz CPD gyrotrons. Each gyrotron delivers about 200–300 kW of microwave power into LHD. The antenna system used here is specially designed for a strongly focused beam. The magnetic field strength and the configuration are selected to have a power deposition as nearly on axis as possible. In addition to

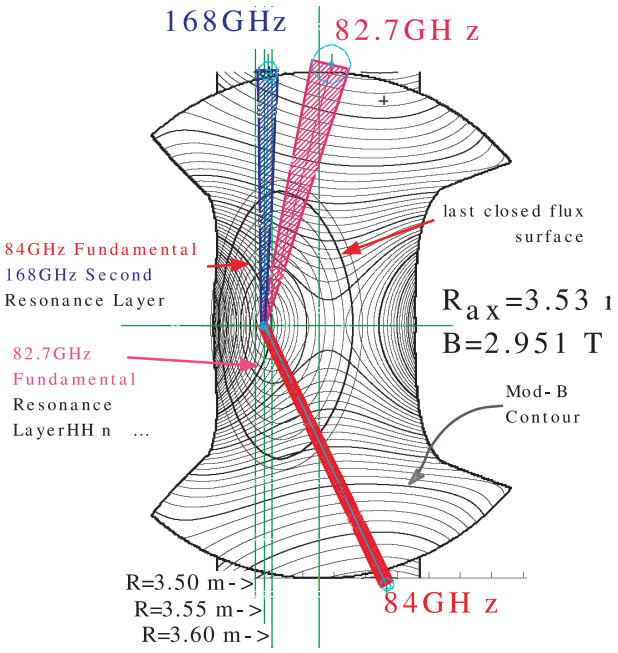

Fig. 1. Flux surfaces and mod-*B* contours in LHD at the vertically elongated cross section. The injected microwave beams from upper and lower antennas are shown. The beam width shown in the figure scales to each beam waist size.

these five antennas, two horizontal injection antennas are available.

The magnetic field strength is selected so as to meet the resonance condition at the injected microwave frequency. The selected magnetic axis is 3.53 m, and the toroidally averaged magnetic field strength on the axis is 2.951 T. The expected power deposition profile estimated by ray tracing, including the weakly relativistic effect, indicates that almost all of the injected power from the upper and lower antennas is concentrated within an average minor radius of $\rho \approx 0.2$.

Figure 2 shows the time evolution of the injected total power, electron density, and stored energy for the highest central electron temperature achieved so far in LHD. Almost 1.2 MW of ECH power is concentrated inside $\rho \approx 0.2$. The two 84-GHz gyrotrons injected 0.7 MW to produce and heat the plasma. After the density and the stored energy attained quasi-steady state, the 168-GHz and 82.7-GHz power were added simultaneously.

Although no additional gas puff was supplied, the density keeps increasing slightly. The high power YAG-Thomson scattering system was used at the times indicated by the arrows in Fig. 2. The electron temperature profiles are shown in Fig. 3. The profile is already sharp in the phase when only the 84-GHz power is injected. The strongly

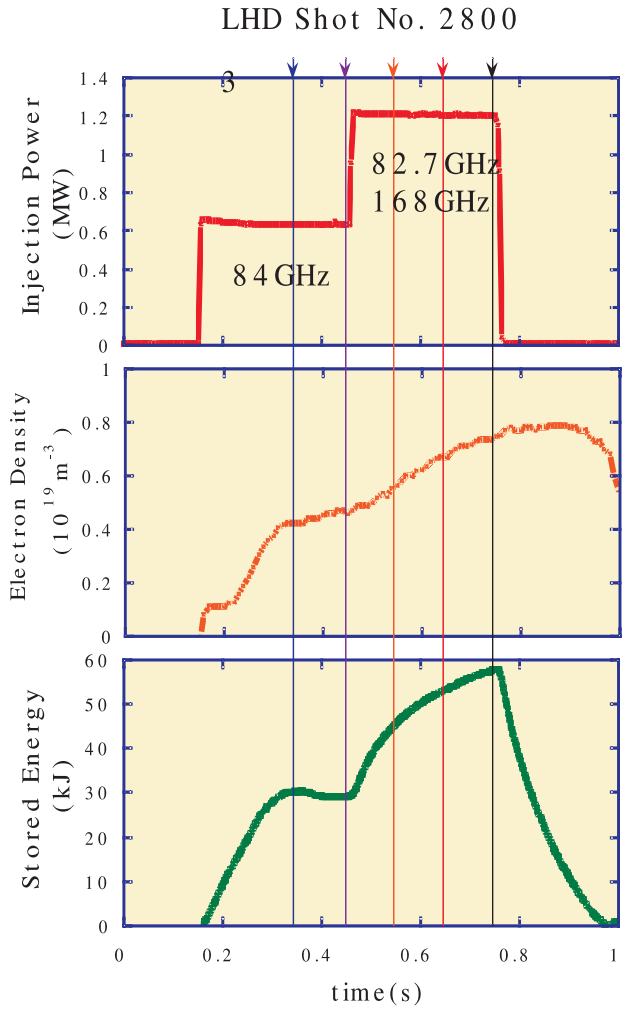

Fig. 2. Time evolution of injected ECH power (top), average electron density (middle), and stored energy (bottom).

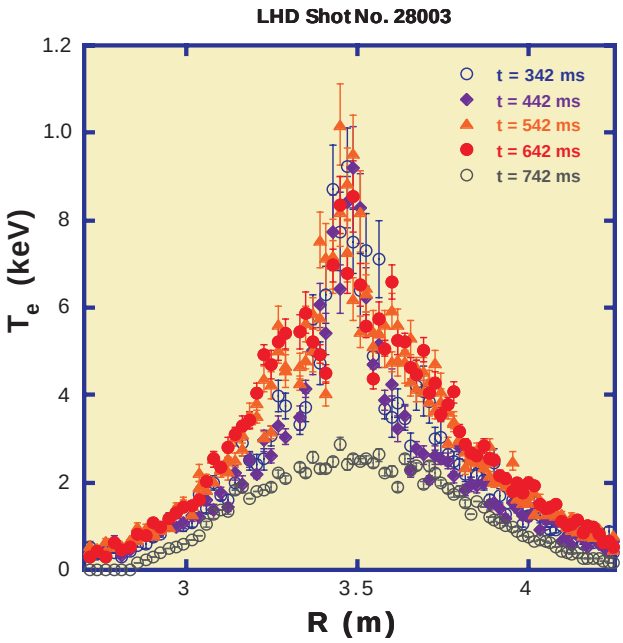

Fig. 3. Electron temperature profile measured by a high power YAG-Thomson scattering at the times indicated by the arrows in Fig. 2.

focused 82.7-GHz power raises the central electron temperature by more than 10 keV. The region where the temperature exceeds 9 keV is limited to an average minor radius less than $\rho \approx 0.1$. These high electron temperature modes appear only when the injected power exceeds a certain threshold level, and this threshold level increases with the electron density.

Because of the low density region, the behavior of the non-thermal electrons is of much interest. The presence of high-energy electrons can affect the power deposition profile and also the confinement. The electron temperature profile shows a steep temperature gradient that resembles those found in plasmas with an internal transport barrier. The presence of the threshold power level and its dependence on the electron density and the focal points are also observed.

These features will be studied in detail by combining the power modulation technique and fine focal point controllability.

Shin Kubo for the LHD Experimental Group
National Institute for Fusion Science
Toki, Gifu 509-5292, Japan
E-mail: kubo@LHD.nifs.ac.jp